



TECHNICAL ARTICLE

Accelerated Diffusion Phenomenon in Ti-B₄C System and its Influence on the Resulting Composites

Lei Jia, Minghao Hou, Chen Zhang, Jin Xu, Shufeng Li, Zhenlin Lu, and Katsuyoshi Kondoh

Submitted: 10 February 2022 / Revised: 31 May 2022 / Accepted: 24 June 2022 / Published online: 19 August 2022

Ti(O)-B₄C diffusion couples and (TiC + TiB)/Ti(O) composites were prepared to study the accelerated diffusion phenomenon and its influence at β transition temperatures (β_t) of Ti matrix. Results show that Ti(O) alloys can be successfully prepared from Ti and TiO₂ powder, and their β_t can be regulated by controlling O contents. Thickness of reaction products in Ti(O)-B₄C reaches the maximum when it is sintered at β_t , indicating that α/β transition of Ti matrix can accelerate the diffusion of atoms inside it. Besides, (TiC + TiB)/Ti(O) composites have the highest size and number of reinforcements when Ti(O)-B₄C powders are sintered at β_t temperature, especially for TiB fiber, but its flexural strength and plasticity are the lowest due to the interface stripping between the coarse reinforcements and matrix.

Keywords accelerated diffusion, mechanical properties, microstructure, powder metallurgy, titanium

1. Introduction

Ti alloys have attracted great attention for the high specific strength, stiffness and excellent corrosion resistance in aviation, aerospace and marine industries and medical instruments (Ref 1-3). However, the strength of pure Ti cannot satisfy the increasing requirements of modern industry, resulting in increasing attempts to explore high-strength Ti alloys by using alloying elements, such as Al, Nb, V and Mo (Ref 3-6). The most commonly used method to prepare Ti alloys is smelting and casting, but the equipment is often very expensive because of the strict requirements for vacuum conditions and crucible to adapt to the high chemical activity of liquid titanium (Ref 2). Besides this, the wear resistance of most Ti alloys is lower than that of Ti composites (Ref 7). Subsequently, the introduction of ceramic phases or intermetallics into Ti matrix is one of the most important ways to improve the strength of Ti materials, and many reinforcements have been successfully added into titanium matrix, such as Al₂O₃, SiC, B₄C, TiC, TiB, TiB₂ and TiN (Ref 8, 9).

Compared with the ex situ method, the ceramic phase or intermetallics introduced by in situ method have great advantages in the interfacial bonding between matrix and reinforcements, which facilitates the load transfer from matrix to reinforcements and can extremely improve the strengthening effect, thus becoming the hot research topic in titanium matrix

composites at present (Ref 9). TiC, TiB and TiB₂ are considered as the most ideal reinforcements for Ti matrix, since their density and thermal expansion coefficient are similar to that of Ti matrix and especially can be introduced by in situ reaction of Ti-B₄C powder system during the consolidation process of Ti matrix composites (Ref 9). As a consequence, (TiC + TiB)/Ti composite prepared by powder metallurgy method from Ti-B₄C powder system is one of the most commonly used methods in the research field of Ti matrix composites due to the abovementioned advantages of in situ reaction and the low chemical activity of Ti matrix at solid state.

As well known, the sintering temperature, always above 1000 °C in most of the published work on Ti-B₄C system, has significant influence on the microstructure and properties of powder metallurgy materials (Ref 9). The fabrication process of (TiC + TiB)/Ti composites can be divided into two stages, viz. the consolidation of Ti matrix and the in situ reaction between Ti and B₄C, both of which depend on the diffusion behavior. According to the classical solid diffusion theory, the higher the temperature is, the higher the diffusion rate will be. Nevertheless, due to the great difference in self-diffusion coefficient between α and β phases, an abnormal accelerated diffusion phenomenon can often be observed near β transition temperature (β_t) of some special metals, which often have hcp structure at room temperature but bcc structure at high temperature, such as Ti, Zr, and Hf (Ref 10-12). This means that the diffusion rate of solid solution atoms in these metals at β_t is even much higher than that at higher temperature. If this accelerated diffusion phenomenon can be utilized, the sintering temperature of Ti-B₄C system can be effectively lowered, which has a great potential in refining the microstructure, energy conservation and emission reduction.

To better understand this accelerated phenomenon and clarify its influence on the microstructure and mechanical properties of the composites, Ti(O) solution alloys were firstly prepared by adding TiO₂ into Ti matrix, and their β_t temperatures were measured by metallographic method. Subsequently, Ti(O)-B₄C diffusion couples were prepared under different temperatures, and the accelerated diffusion phenomenon at β_t temperature was studied in detail. Finally, (TiC + TiB)/Ti(O)

Lei Jia, Minghao Hou, Chen Zhang, Jin Xu, Shufeng Li, and Zhenlin Lu, School of Materials Science and Engineering, Xi'an University of Technology, Xi'an 710048, China; and Katsuyoshi Kondoh, Joining and Welding Research Institute, Osaka University, Osaka 567-0047, Japan. Contact e-mail: xautjialei@hotmail.com.

composites were prepared from Ti(O)-B₄C powder system by sintering near β_t temperatures, and the influence of accelerated diffusion on microstructure and mechanical properties was investigated.

2. Experimental Details

2.1 Determination of Decomposition Temperature of TiO₂ in Ti

Pure titanium powder ($\geq 99.5\%$, 20 μm) and TiO₂ powder ($\geq 99.9\%$, 1 μm) were used as raw materials. Firstly, Ti-TiO₂ powder mixture with 5 wt.% TiO₂ was prepared by using a rocking milling machine, where ZrO₂ balls were used and the ball-to-powder ratio is 1:2. Then, the powder mixture was sintered by a spark plasma sintering (SPS) machine at 500, 600, 700 and 800 °C for 30 min, respectively. The whole sintering process was carried out in a vacuum environment lower than 6 Pa at an axial pressure of 30 MPa. Subsequently, microstructure and phase composition were characterized by scanning electron microscopy (SEM) and x-ray diffraction (XRD). Hardness was determined by micro-Vickers hardness tester with load of 50gf and duration time of 30 s, and density was determined by Archimedes drainage method. Based on the above results, the decomposition temperature of TiO₂ in Ti matrix can be determined finally.

2.2 Preparation of Ti(O) Alloys and their β_t Measurement

Ti(O) solid solution alloys were prepared by adding TiO₂ powder with different contents into pure Ti powder to adjust the β transformation temperature of titanium matrix. First of all, Ti and TiO₂ powder were mixed by rocking mill machine (RM-05), and the amount of TiO₂ powder added was calculated according to the content of O introduced, viz. 0, 0.25 and 0.5 wt.% respectively, where the parameters for powder mixing were the same as that described in Sect. 2.1. Subsequently, the mixed powder was sintered by SPS machine at 1000 °C for 30 min, under the same environment and pressure as mentioned above. Finally, the sintered block was cut into cylindrical samples with $\phi 10 \times 12$ mm for β_t measurement.

β_t of Ti(O) solid solution alloy was determined by metallographic method, referring to the National Standard of China (GB/T23605-2009) (Ref 13), which was carried out in a calibrated L-T1250S tubular furnace. Before the experimental measurement, β_t of Ti(O) solid solution alloy was pre-evaluated according to empirical formula (Ref 14), based on the contents of oxygen and nitrogen measured by Oxygen–Nitrogen–Hydrogen Analyzer (EMGA-830). Firstly, the samples were heated to different temperatures around the pre-evaluated β_t with a heating rate of 10 °C min⁻¹ and then held for 30 min at the target temperature under an argon protection environment. Secondly, the samples were quickly quenched into a water tank with a temperature below 25 °C within 5 s. Finally, metallographic investigation was carried out, and then the corresponding water-quenching temperature is confirmed as the β_t of Ti(O) solid solution alloy when the volume fraction of residual primary α -Ti phase is less than 5%.

2.3 Preparation and Characterizations of Ti(O)-B₄C Diffusion Couple

In order to study the influence of sintering temperature on the reaction behavior between Ti(O) and B₄C, Ti(O)-B₄C diffusion couples were prepared as follows. Firstly, B₄C powder ($\geq 99.9\%$, 0.5 μm) was used as the raw material to prepare block sample with $\phi 15 \times 5$ mm by SPS sintered at 1800 °C for 15 min, where the other processing parameters were the same as above. The B₄C block was polished and cleaned by acetone solution on surface and then placed onto the inferior punch of SPS module. Subsequently, mixture of pure titanium and TiO₂ with nominal oxygen content 0, 0.25 and 0.5 wt% was filled into graphite mold and sintered by SPS. The assembling method of graphite dies and raw materials were described in our previous work (Ref 15). At the beginning of sintering, the sample was held at 800 °C for 30 min, enabling TiO₂ to decompose and dissolve into Ti matrix to form Ti(O) alloy. After that, the sintering temperature was further increased to around the β_t of Ti(O) alloys (β_t-90 , β_t-40 , β_t and β_t+30 °C) and held for 0, 0.5, 1 and 1.5 h, respectively. For Ti(O) alloy with a given oxygen content, 16 Ti(O)-B₄C diffusion couples were prepared by sintering at different temperatures and time lengths under the same environment and pressure as above. Finally, metallurgical investigation was performed on the longitudinal section of diffusion couples, and then the phase composition of products was studied by TEM selected-area electron diffraction (SAED) analysis, while the thickness of diffusion reaction layer was measured through SEM images from five different locations.

2.4 Preparation and Characterizations of (TiC + TiB)/Ti(O) Composites

In order to verify the influence of accelerated diffusion behavior near β_t on the microstructure and properties of composites in Ti-B₄C system, (TiC + TiB)/Ti(O) composites were prepared from the mixture of Ti, TiO₂ and B₄C powder. Firstly, three kinds of raw powder were weighed according to 0.25wt. O and 1.61wt.% B₄C and then mixed uniformly by rocking milling machine. Then, the powder mixture was sintered by the similar sintering craft to that used to prepare Ti(O)-B₄C diffusion couple, viz. sintering at 800 °C for 30 min to facilitate the formation of Ti(O) solid solution from TiO₂ and Ti firstly, and then further sintering around the β_t temperature of Ti(O) matrix (β_t-90 , β_t-40 , β_t and β_t+30 °C) for 1 h to ensure the full reaction between Ti(O) and B₄C powder. Finally, microstructure and phase composition of (TiC + TiB)/Ti(O) composites were investigated by XRD, SEM and EPMA, respectively, while the mechanical properties were studied by three-point bending test according to the National Standard GB/T232-2010 (Ref 16), where the sample size was 28(L) \times 3(b) \times 5(h) mm and the span (l) is 20 mm, and the flexure strength was calculated as follows:

$$\sigma_{bb} = \frac{3P_b \times l}{2bh^2} \quad (\text{Eq 1})$$

where P_b is the maximum load.

3. Results and Discussion

3.1 Decomposition and Solution Behavior of TiO₂ in Ti Matrix

Figure 1 shows XRD patterns of Ti-TiO₂ mixed powder sintered at different temperatures. Diffraction peaks corresponding to α -Ti and TiO₂ phase can be easily detected from the original Ti-TiO₂ powder mixture, indicating that no alloying occurred during the mixing process. When sintering temperature is reached at 500 °C, one diffraction peak ($2\theta = 25.5^\circ$) corresponding to TiO₂ phase weakens and the other peak ($2\theta = 48^\circ$) disappears, while a new peak ($2\theta = 29.5^\circ$) corresponding to Ti₇O₁₃ phase starts to appear. With the increase in sintering temperature, all the peaks corresponding to TiO₂ phase disappear, and the intensity of the peak corresponding to Ti₇O₁₃ phase increases first and then decreases, suggesting that TiO₂ has already started to decompose at the temperature above 500 °C, and the intermediate product is Ti₇O₁₃. When the sintering temperature is further increased to 800 °C, all diffraction peaks only correspond to α -Ti. Moreover, the diffraction peaks corresponding to α -Ti gradually move toward the left hand with the increase in sintering temperature, further demonstrating the decomposition of TiO₂ and the solid solution of O elements into Ti matrix.

3.2 Determination on the β_t of Ti(O) Alloys

Table 1 shows the oxygen and nitrogen contents of the three kinds of Ti(O) alloys prepared by adding different contents of TiO₂ into Ti matrix. For pure Ti materials without TiO₂, the O content is about 0.307%, which is basically in accordance with that provided by powder manufacturers, indicating that there is no obvious oxidation during sintering. For the Ti(O) alloys, the increase in O content is also nearly equal to the designed O content, indicating that TiO₂ is decomposed and dissolved into titanium matrix. In the meantime, the contents of N in three alloys are basically similar and remain at a low level, which also suggests that the vacuum condition is high enough for the sintering of Ti materials. On this basis, the β_t of Ti(O) solid solution alloys with different compositions can be mainly

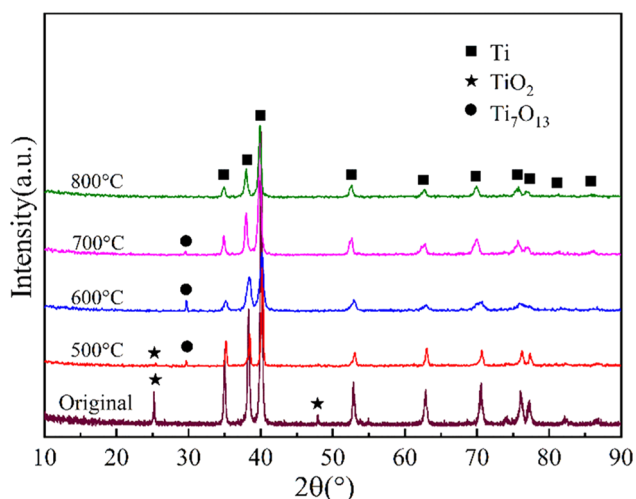


Fig. 1 XRD patterns of original Ti-TiO₂ powder mixture as well as that after being sintered at different temperatures for 30 min

predicted by the following equation (Ref 14), and the result is also summarized in Table 1.

$$\beta_t = 885^\circ\text{C} + 200 \times [\text{O}] \% + 550 \times [\text{N}] \% \quad (\text{Eq 2})$$

where [O] and [N]% are the mass percentage of O and N in Ti alloy, respectively. Especially, the formula (2) is only applicable when the oxygen content is less than 1% and the N content is less than 0.5%.

In order to accurately determine the β_t of Ti(O) solid solution alloys with different oxygen contents, water-quenching experiments were carried out near theoretical transition temperature, and the typical microstructure at the temperature before and after the end of α/β transition is shown in Fig. 2. According to national standard of metallographic method (Ref 13), the α/β transition temperature is characterized by the residual volume content of primary α phase which is less than 5%, as shown in Table 1. It is obvious that the β_t of Ti(O) solid solution alloys increase significantly with the increase in O content, and the increment remains relatively stable (70–80 °C). However, the measured values are always higher than the theoretical ones due to the very small amount of unknown impurities, since the nominal composition of purity titanium powder is 99.5 wt.% Ti and 0.3 wt.% O.

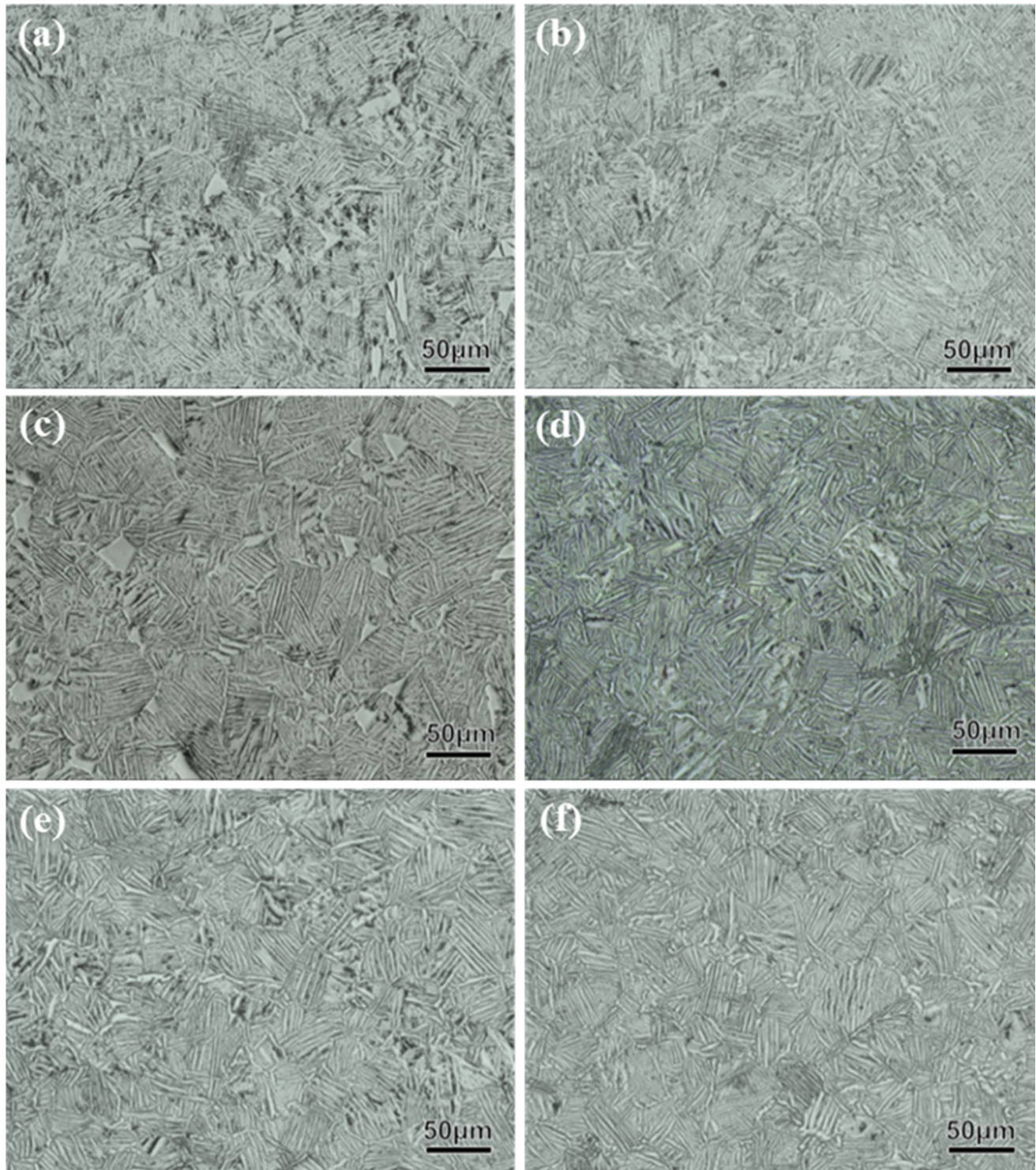
3.3 Diffusion Behavior of Ti-B₄C System Near β_t

Figure 3 shows the results of microstructure characterizations on the Ti-B₄C diffusion couple sintered at 900 °C for 30 min. From the SEM image, it can be found that there is a dense layer between Ti and B₄C, and some whiskers and particles dispersed in the Ti matrix, as shown in Fig. 3(a). TEM analysis in the yellow area in SEM image shows that there are a large number of reinforcements in the Ti matrix and the morphologies present to be particle- and whisker-like. Selected-area diffraction patterns suggest that the reinforcements are TiB and TiC, agreeing well with other related work (Ref 17). Although TEM specimen cannot be prepared on the dense layer since it is too brittle to be thinned by ion thinning method, the phase composition of such a layer can be identified as TiB₂ according to our previous work (Ref 18, 19), where the diffusion and reaction behavior of Ti-B₄C system can also be found; namely, B and C atoms diffuse into Ti matrix to form TiB and TiC along with the decomposition of B₄C, and then Ti atom diffuses into B₄C block to form TiB₂ layer via the vacancies left by the out diffusion of B and C. Therefore, it is equivalent to characterize the diffusion and reaction degree of Ti-B₄C by using the thickness of the layer containing TiB and TiC or that of the dense TiB₂ layer.

Considering that the thickness of TiB and TiC layer is difficult to measure, the thickness of the TiB₂ layer is used to study the influence of sintering temperature and time length on the reaction behavior of Ti(O)-B₄C, as shown in Fig. 4. It is clear that the influence of temperature and time length on the thickness of reaction layer always obey the same law regardless of the O content in Ti matrix. The thickness of reaction layer always increases with the prolongation of sintering time at first and then slightly decreases with the increase in temperature and reaches the maximum value when sintering at the β_t of Ti(O) matrix, which can also be demonstrated by the inserts in Fig. 4. Obviously, there is an accelerated diffusion phenomenon near β_t of titanium matrix, which is inconsistent with traditional solid-state diffusion theory. To better clarify such an abnormal

Table 1 O/N contents of Ti(O) alloys and their theoretical β transition temperature

Nominal composition	O, %	N, %	Theoretical β_t temperature, °C	Real β_t temperature, °C
Ti	0.307	0.003	948	985
Ti-0.25wt.%O	0.551	0.003	997	1065
Ti-0.5wt.%O	0.788	0.005	1045	1135

**Fig. 2** Typical microstructure of Ti(O) alloy quenched from the temperature before and after the end of β transition, (a) 980 and (b) 990 °C for pure Ti, (c) 1060 and (d) 1070 °C for Ti + 0.25wt.% O, (c) 1130 and (d) 1140 °C for Ti + 0.50wt% O, respectively

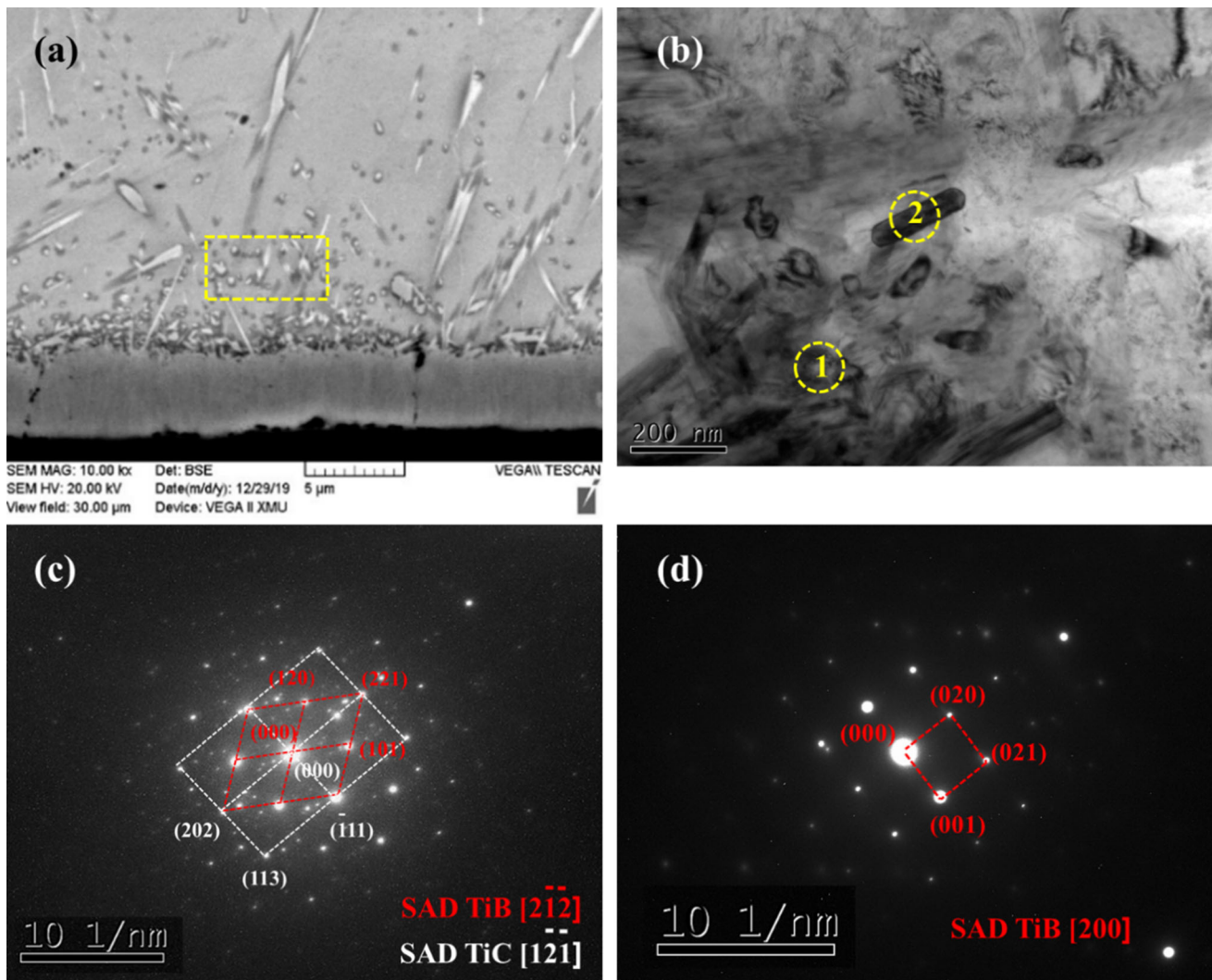


Fig. 3 Microstructure characterizations on the Ti-B₄C diffusion couple prepared by sintering at 900 °C for 30 min, (a) SEM image, (b) TEM bright-field image on the yellow rectangle area, (c) and (d) SAED patterns on the areas marked by 1 and 2, respectively (Color figure online)

phenomenon, the diffusion behavior is analyzed from the viewpoint of diffusion kinetics.

For solid diffusion, the growth of diffusion layer is usually described by the power law growth rule (Ref 14).

$$\delta = Dt^n \quad (\text{Eq 3})$$

where δ is the thickness of diffusion layer, D is the reaction rate constant, n is the kinetic factor and t is the growth time. Equation 3 is taken by logarithm and then obtains:

$$\ln \delta = n \ln t + \ln D \quad (\text{Eq 4})$$

Taking the data in Fig. 4 into Eq. 4, the results can be seen in Fig. 5. It can be seen that, for Ti(O)-B₄C diffusion couples with different oxygen contents, there is always a good linear logarithm relationship between the thickness of TiB₂ layer and holding time further proving the rationality of power law equation. The values of n and D obtained by fitting the experimental results are summarized in Table 2, and all the Pearson's correlation coefficients are higher than 0.85, indicating a remarkable linear relationship. It can be found that n values are all below 0.5 in the temperature range studied, indicating that reaction between Ti(O)-B₄C is mainly controlled

by diffusion (Ref 20). Furthermore, although the increase in sintering temperature always leads to the increase in D values, the maximum value of the Ti(O)-B₄C with different oxygen content is always obtained at the time of sintering at β_t , which is the key evidence for the abnormal increase in the reaction layer thickness at transition temperature of Ti matrix. It is a fact that this accelerated diffusion phenomenon near transition temperature can be attributed to isomeric transformation of Ti matrix and the significant increase in the self-diffusion rate difference between α and β crystal structure (Ref 21).

3.4 Effect of Sintering at β_t on the Synthesized Composites from Ti-B₄C System

Figure 6 shows the XRD patterns of the composites as well as the compared alloy matrix sintered near the β_t of Ti matrix. Compared with the Ti-0.25%O solution alloy, the diffraction peaks corresponding to TiC and TiB can be easily seen from the XRD patterns, indicating that (TiC + TiB)/Ti(O) composites can be successfully synthesized from Ti-0.25%O and B₄C powder system. However, the similar XRD patterns cannot provide sufficient information about the influence of sintering temperature on the phase composition of (TiC + TiB)/Ti(O)

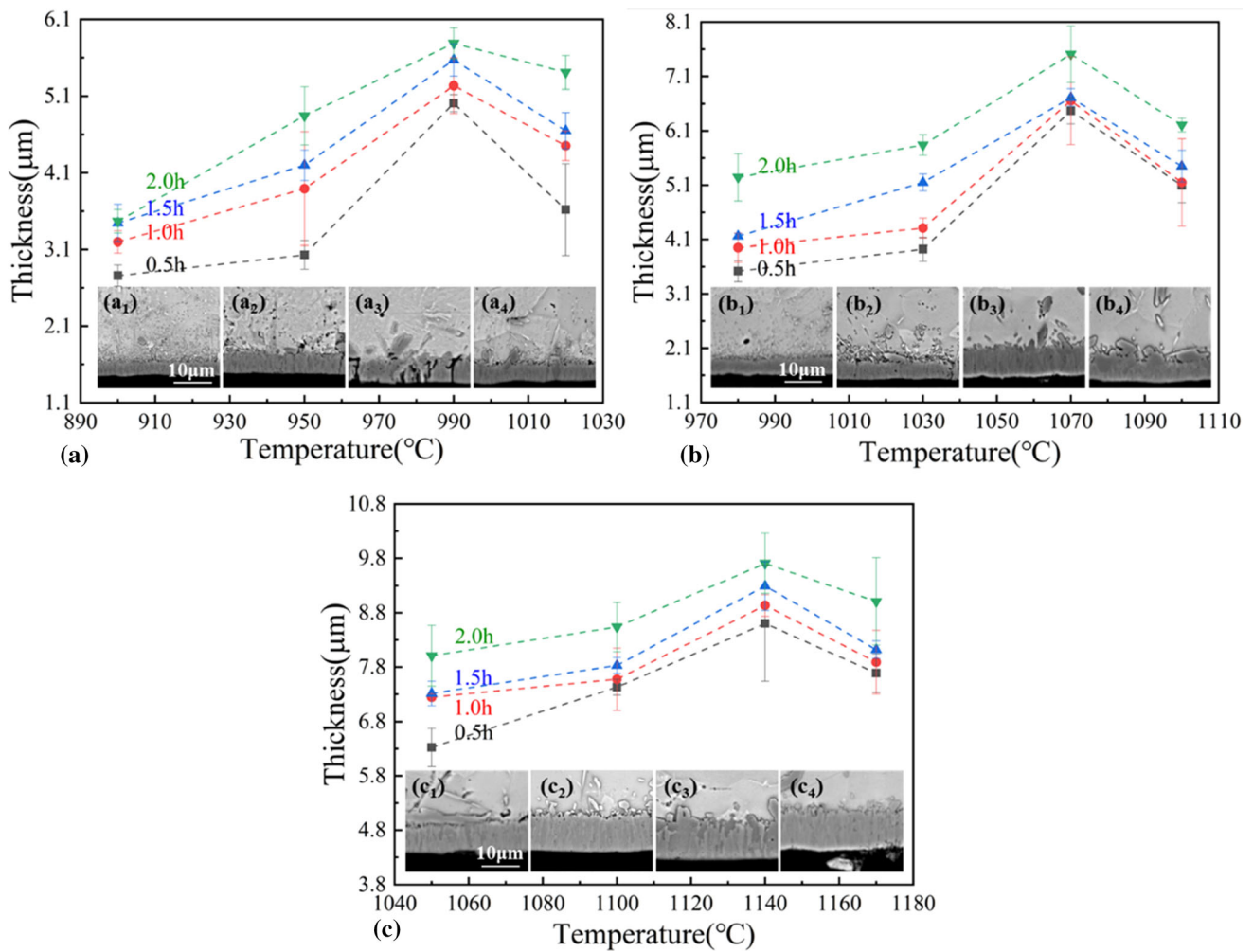


Fig. 4 Variation of the thickness of TiB_2 layer in $Ti(O)-B_4C$ diffusion couples under different temperatures and holding time, where the nominal oxygen contents are (a) 0, (b) 0.25 and (c) 0.5%, respectively

composites, since the content of TiC and TiB is not high enough to cause significant differences on the intensity of the XRD peaks. On the other hand, XRD patterns agree well with the results of TEM analysis on diffusion couples and other relative works (Ref 7, 22, 23).

Figure 7 shows the microstructure of $(TiC + TiB)/Ti(O)$ composites prepared by sintering at different temperatures near β_t of $Ti(O)$ matrix. It can be found that the morphologies of the different composites are similar to each other, and there are many particle-like and some whisker-like reinforcements in the matrix, which are TiC particles and TiB whiskers according to the XRD patterns and our previous work as well as other related works (Ref 23, 24). On the whole, both the size and number of reinforcements increase with the increasing sintering temperature, especially the TiB whiskers. When the sintering temperature is $980^{\circ}C$, only several whiskers can be found, and they are too small to be easily seen, as seen in Fig. 7(a). When the sintering temperature is the β_t of $Ti(O)$ matrix, the TiB whiskers grow larger, even larger than that at the highest temperature, as shown in Fig. 7(c) and (d). Such a result indicates that sintering at the β_t of Ti matrix facilitates the diffusion and reaction between Ti and B_4C . It is worth mentioning that the portion of TiC particles and TiB whiskers phase in SEM images is not accordance with their theoretical portion in chemical reaction,

since TiB can only present whisker-like shape on special section.

Figure 8 shows the L-D curves of three-point bending test on $(TiC + TiB)/Ti(O)$ composites sintered at different temperatures near β_t of $Ti(O)$ matrix. Compared with $Ti(O)$ solution matrix without any reinforcements, the slopes of the L-D curves (meaning the elastic modulus) of $(TiC + TiB)/Ti(O)$ composite increase but the plasticity decreases, which is due to the introduction of high modulus TiC particles and TiB whiskers by in situ reaction. However, with the increase in sintering temperature, both the strength and plasticity of the composites decrease significantly. When the sintering temperature is higher than $1030^{\circ}C$, the strength of the $(TiC + TiB)/Ti(O)$ composites (976 and 1168 MPa) is even lower than that of $Ti(O)$ matrix (1448 MPa), especially when $Ti(O)-B_4C$ is sintered at the β_t of $Ti(O)$ matrix, namely $1070^{\circ}C$.

In order to clarify the reasons for the decrease of strength and plasticity caused by the increase in sintering temperature, the fracture morphologies of the matrix alloy and composites were observed, as shown in Fig. 9. For the $Ti(O)$ solution alloy, large cleavage surface, obvious cleavage steps and some dimples can be found, indicating that the alloy presents a mixture of ductile and brittle fracture, which agrees well with the result of bending test. However, for the $(TiC + TiB)/Ti(O)$

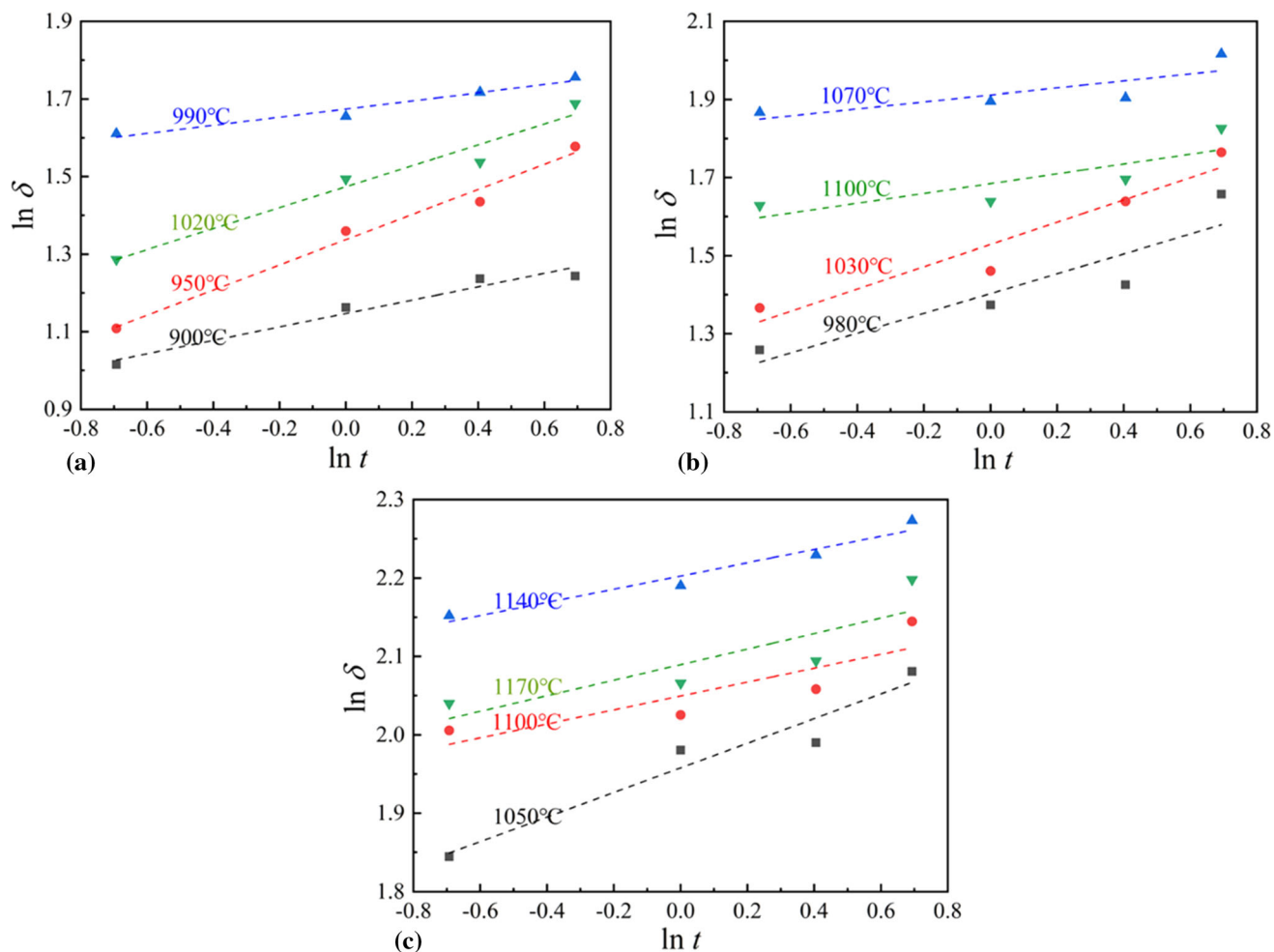


Fig. 5 Relationships between $\ln \delta$ and $\ln t$ for Ti(O)-B₄C diffusion couples with oxygen contents (a) 0, (b) 0.25 and (c) 0.5%, respectively

Table 2 Values of n and D of Ti(O)-B₄C diffusion couples with different O content and prepared by sintering at different temperatures

O content, wt.%	Temperature, °C	N	$D(10^{-7} \text{ m s}^{-0.2})$	Pearson's correlation coefficient
0	900	0.17	6.14	0.98
	950	0.32	7.42	0.99
	990	0.10	10.33	0.98
	1020	0.27	8.46	0.98
0.25	980	0.25	7.88	0.91
	1030	0.28	8.98	0.96
	1070	0.09	13.13	0.85
	1100	0.13	10.43	0.87
0.5	1050	0.16	13.80	0.96
	1100	0.09	15.10	0.87
	1140	0.08	17.55	0.97
	1170	0.10	15.72	0.85

composites, large cleavage surfaces are substituted by coarse and rugged surfaces dispersed with TiC particles and TiB whiskers, and dimples cannot be observed anymore. With the increase in sintering temperature, more and more coarse TiB whiskers or their traces appear on the fracture surface, especially at 1070 and 1100 °C, as shown in Fig. 9 (d) and (e).

The smooth fracture trace of the TiB whiskers means the poor bonding between TiB and Ti(O) matrix, and thus the coarser the TiB whiskers are, the worse the strength of the composites will be. This is why the strength of the (TiC + TiB)/Ti(O) composite decreases with the increase in sintering temperature as shown in Fig. 8.

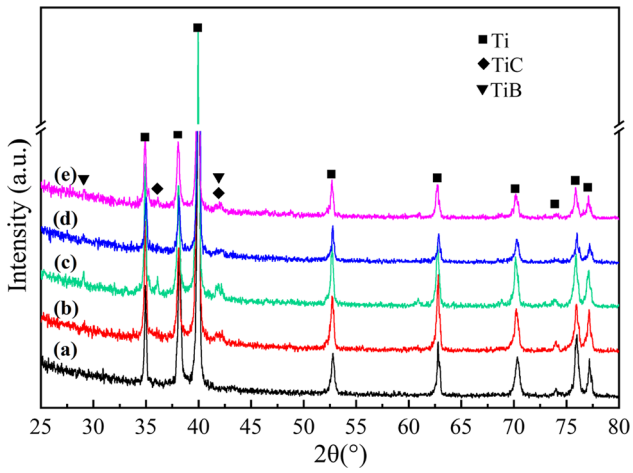


Fig. 6 XRD patterns of (a) Ti-0.25wt%O alloy and (TiC_p + TiB_w)/Ti(O) composites prepared by sintering at (b) 980, (c) 1030, (d) 1070 and (e) 1100 °C, respectively

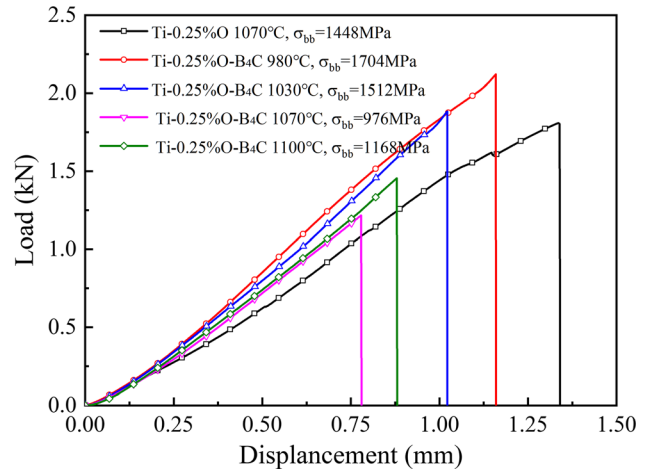


Fig. 8 L-D curves of Ti(O) alloy matrix and (TiC + TiB)/Ti(O) composites prepared by sintering at different temperatures

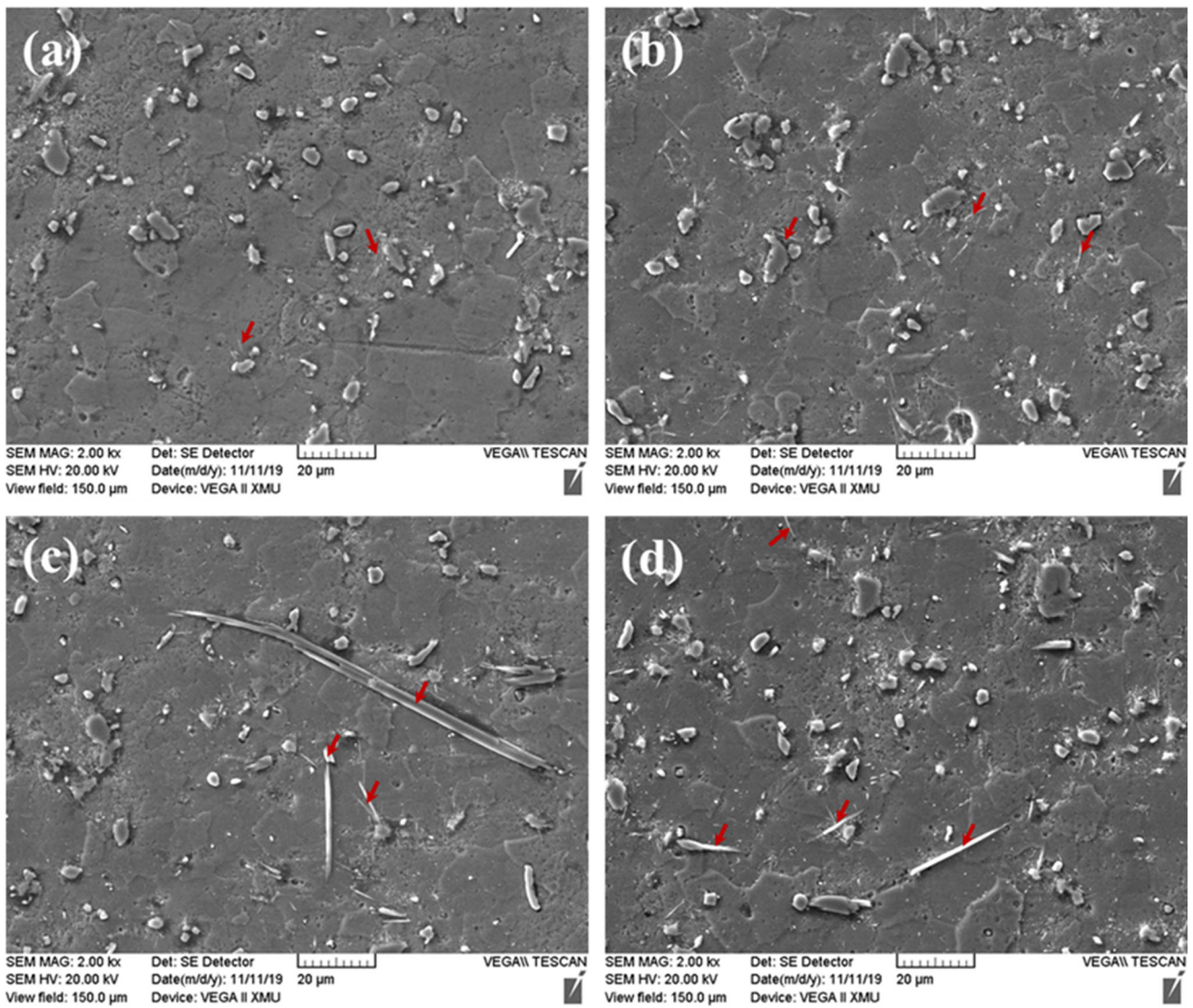


Fig. 7 Microstructures of (TiC + TiB)/Ti(O) composites prepared by sintering at (a) 980, (b) 1030, (c) 1070 and (d) 1100 °C, respectively

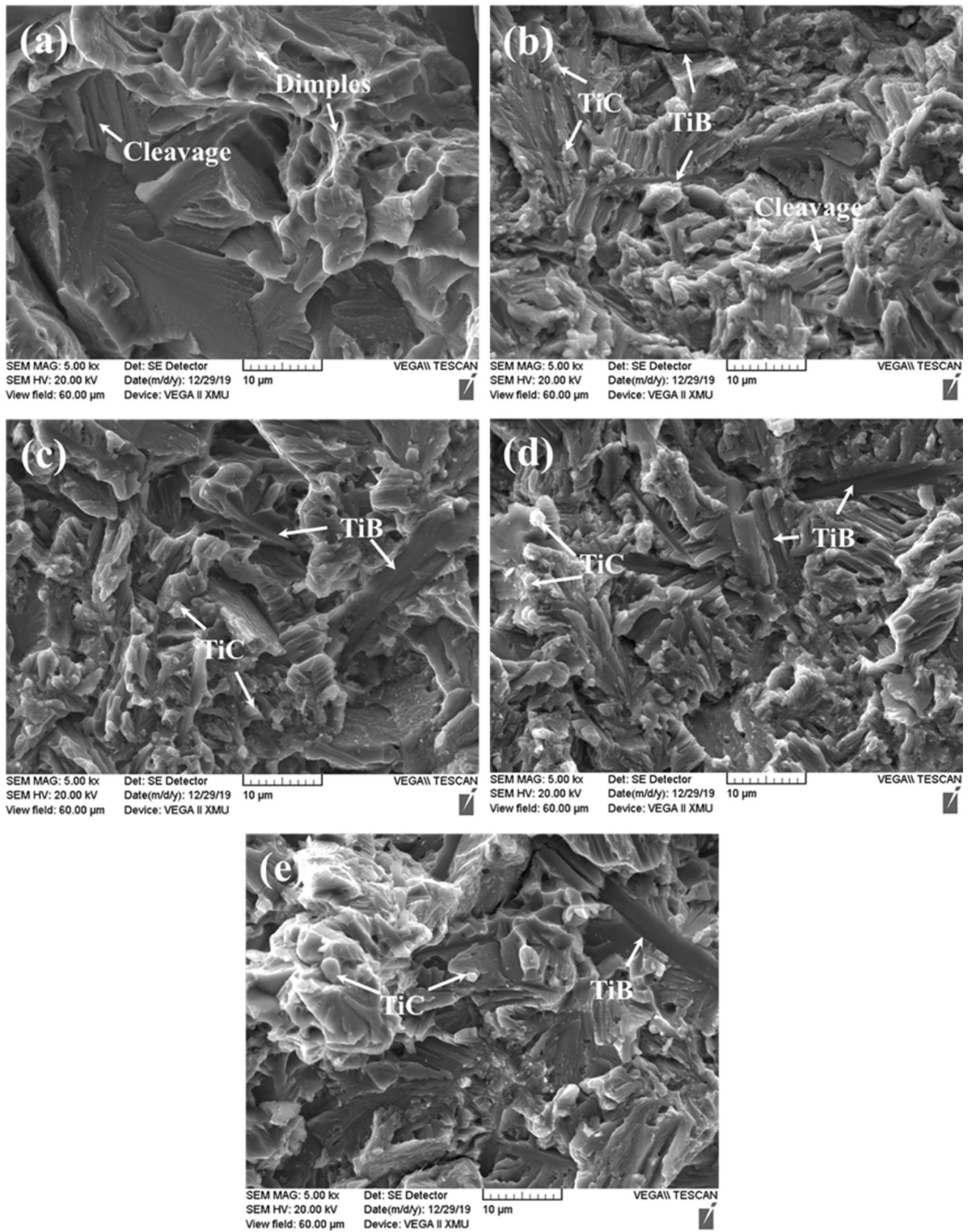


Fig. 9 Fracture morphologies of (a) Ti(O) matrix and (TiC_p + TiB_w)/Ti(O) composites prepared by sintering at (b) 980, (c) 1030, (d) 1070 and (e) 1100 °C, respectively

4. Conclusion

- (1) Ti(O) solid solution alloys can be prepared by powder metallurgy method from Ti and TiO₂ powder mixture at the temperature above 800 °C, and their β_t increases with the increase in oxygen content.
- (2) The thickness of the diffusion and reaction layer in Ti(O)-B₄C diffusion couple generally increases with the increasing sintering temperature, but reaches the maximum value at the β_t temperature of Ti(O) alloys, demonstrating the existence of accelerated diffusion phenomenon in Ti alloys.
- (3) Sintering temperature at β_t of Ti(O) matrix can result in the excessive growth of TiC and TiB reinforcements, and the decrease in both strength and elongation of (TiC + TiB)/Ti(O) composites, which can be attributed to the previous fracture of the interface between Ti and coarse TiB whiskers.

Acknowledgments

The authors are grateful to National Nature Science Foundation of China (51601143/51875453) for finance support.

Conflict of interests

The authors have no competing interests to declare that are relevant to the content of this article.

References

1. L. Jia, J.X. Chen, Z.L. Lu, S.F. Li, J. Umeda, and K. Kondoh, Preparation of Si and O Co-Solution Strengthened Ti Alloys by Using Rice Husks as SiO₂ Resource and Quantitative Descriptions on Their Strengthening Effects, *Mater. Res. Express*, 2018, **5**(4), p 046524
2. Y.S. Zhang, X. Wang, W. Zhang, W.T. Huo, J.J. Hu, and L.C. Zhang, Elevated Tensile Properties of Ti-O Alloy with a Novel Core-Shell Structure, *Mater. Sci. Eng. A*, 2017, **696**, p 360–365
3. Y.K. Chou, L.W. Tsay, and C. Chen, Effects of Aging Treatments on the Mechanical Behavior of Ti-15V-3Cr-3Sn-3Al Alloy, *J. Mater. Eng. Perform.*, 2015, **24**(9), p 3365–3372
4. J.Q. Qi, Y. Chang, Y.Z. He, Y.W. Sui, F.X. Wei, Q.K. Meng, and Z.J. Wei, Effect of Zr, Mo and TiC on Microstructure and High-Temperature Tensile Strength of Cast Titanium Matrix Composites, *Mater. Des.*, 2016, **99**, p 421–426
5. S. Zeng, A. Zhao, H. Jiang, and Y. Ren, Flow Behavior and Processing Maps of Ti-44.5Al-3.8Nb-1.0Mo-0.3Si-0.1B Alloy, *J. Alloys Compd.*, 2017, **698**, p 786–793
6. W. Wang, H. Zhou, Q. Wang, Y. Gao, and K. Wang, Influence of Mechanical Alloying and Sintering Temperature on the Microstructure and Mechanical Properties of a Ti-22Al-25Nb Alloy, *J. Mater. Eng. Perform.*, 2020, **29**(3), p 1686–1695
7. B.J. Choi, I.Y. Kim, Y.Z. Lee, and Y.J. Kim, Microstructure and Friction/Wear Behavior of (TiB+TiC) Particulate-Reinforced Titanium Matrix Composites, *Wear*, 2014, **318**, p 68–77
8. A. Sabahi Namini, M. Shahedi Asl, and S.A. Delbari, Influence of Sintering Temperature on Microstructure and Mechanical Properties of Ti-Mo-B₄C Composites, *Met. Mater. Int.*, 2021, **27**(5), p 1092–1102
9. M. Yi, X. Zhang, G. Liu, B. Wang, H. Shao, and G. Qiao, Comparative Investigation on Microstructures and Mechanical Properties of (TiB+TiC)/Ti-6Al-4V Composites from Ti-B₄C-C and Ti-TiB₂-TiC Systems, *Mater. Charact.*, 2018, **140**, p 281–289
10. Y. Zheng, R.E.A. Williams, G.B. Viswanathan, W.A.T. Clark, and H.L. Fraser, Determination of the Structure of α - β Interfaces in Metastable β -Ti Alloys, *Acta Mater.*, 2018, **150**, p 25–39
11. H.J. Lu, H. Wu, N. Zou, X.G. Lu, Y.L. He and D. Morgan, First-Principles Investigation on Diffusion Mechanism of Alloying Elements in Dilute Zr Alloys, *Acta Mater.*, 2018, **154**, p 161–171
12. A.V. Ruban, V.I. Baykov, B. Johansson, V.V. Dmitriev, and M.S. Blanter, Oxygen and Nitrogen Interstitial Ordering in Hcp Ti, Zr, and Hf: An Ab Initio Study, *Phys. Rev. B Condens. Matter Mater. Phys.*, 2010, **82**(13), p 1–10
13. National Standard of the People's Republic of China GB/T23605–2009, Method for determination of β transformation temperature of Ti alloy (in Chinese)
14. Y.T. Li, L. Geng, B. Xu, A.B. Li, and G.S. Wang, Measurement and Analysis of Phase Transformation Temperature of TC11 Titanium Alloy, *Rare Metal.*, 2006, **30**(2), p 231–234
15. L. Jia, J. Xu, and S.Z.H.K. feng Lilin LuXieKondoh, Reaction Kinetics of Cu–Ni and B₄C in Cu–Ni Alloy under Solid-State Sintering, *Mater. Sci. Technol.*, 2020, **36**(6), p 759–764
16. National Standard of the People's Republic of China GB/T232–2010, Testing method for bending of metallic materials (in Chinese)
17. L. Jia, X. Li, K. Kondoh, B. Chen, S. Li, J. Umeda, and Z. Lu, Hybrid Effect of TiC_p and TiB_w Co-Strengthening Ti Matrix Composites Prepared by Spark Plasma Sintering and Hot Extrusion, *Mater. Charact.*, 2019, **151**, p 6–14
18. L. Jia and S.H.B.K. feng LiImaiChenKondoh, Size Effect of B₄C Powders on Metallurgical Reaction and Resulting Tensile Properties of Ti Matrix Composites by In-Situ Reaction from Ti-B₄C System under a Relatively Low Temperature, *Mater. Sci. Eng. A*, 2014, **614**, p 129–135
19. L. Jia, B. Chen, S.F. Li, H. Imai, M. Takahashi, and K. Kondoh, Stability of Strengthening Effect of in Situ Formed TiC_p and TiB_w on the Elevated Temperature Strength of (TiC_p + TiB_w)/Ti Composites, *J. Alloys Compd.*, 2014, **614**, p 29–34
20. H.Y. Li, X.F. Wang, D.D. Wei, J.D. Hu, and Y.H. Li, A Comparative Study on Modified Zerilli-Armstrong, Arrhenius-Type and Artificial Neural Network Models to Predict High-Temperature Deformation Behavior in T24 Steel, *Mater. Sci. Eng. A*, 2012, **536**, p 216–222
21. B. Sarma and K.S. Ravi Chandran, Accelerated Kinetics of Surface Hardening by Diffusion near Phase Transition Temperature: Mechanism of Growth of Boride Layers on Titanium, *Acta Mater.*, 2011, **59**(10), p 4216–4228
22. D.R. Ni, L. Geng, J. Zhang, and Z.Z. Zheng, Effect of B₄C Particle Size on Microstructure of in Situ Titanium Matrix Composites Prepared by Reactive Processing of Ti-B₄C System, *Scr. Mater.*, 2006, **55**(5), p 429–432
23. L. Jia, C. Zhang, K. Kondoh, R. Niu, B. Chen, S. Li, and Z. Lu, Obvious Yielding Phenomenon and Selective Fracture Behavior in Powder Metallurgy (TiC_p+TiB_w)/Ti Composites, *J. Mater. Res. Technol.*, 2020, **9**(5), p 10184–10188
24. D.R. Ni, L. Geng, J. Zhang, and Z.Z. Zheng, Fabrication and Tensile Properties of in Situ TiB_w and TiC_p Hybrid-Reinforced Titanium Matrix Composites Based on Ti-B₄C-C, *Mater. Sci. Eng. A*, 2008, **478**, p 291–296

Publisher's Note Springer Nature remains neutral with regard to jurisdictional claims in published maps and institutional affiliations.

Springer Nature or its licensor holds exclusive rights to this article under a publishing agreement with the author(s) or other rightsholder(s); author self-archiving of the accepted manuscript version of this article is solely governed by the terms of such publishing agreement and applicable law.